

This discussion paper is/has been under review for the journal Climate of the Past (CP).
Please refer to the corresponding final paper in CP if available.

An optimized multi-proxy, multi-site Antarctic ice and gas orbital chronology (AICC2012): 120–800 ka

L. Bazin¹, A. Landais¹, B. Lemieux-Dudon², H. Toyé Mahamadou Kele²,
D. Veres^{3,4}, F. Parrenin³, P. Martinerie³, C. Ritz³, E. Capron⁵, V. Lipenkov⁶,
M.-F. Loutre⁷, D. Raynaud³, B. Vinther⁸, A. Svensson⁸, S. O. Rasmussen⁸,
M. Severi⁹, T. Blunier⁸, M. Leuenberger¹⁰, H. Fischer¹⁰, V. Masson-Delmotte¹,
J. Chappellaz³, and E. Wolff⁵

¹Laboratoire des Sciences du Climat et de l'Environnement (LSCE), Gif-sur-Yvette, France

²Laboratoire Jean Kuntzmann, Grenoble, France

³Laboratoire de Glaciologie et Geophysique de l'Environnement, CNRS-UJF,
St. Martin d'Hères, France

⁴Institute of Speleology, Romanian Academy, Cluj-Napoca, Romania

⁵British Antarctic Survey, Cambridge, UK

⁶Arctic and Antarctic Research Institute, St. Petersburg, Russia

⁷Université catholique de Louvain, Georges Lemaître Center for Earth
and Climate Research, Belgium

⁸Centre for Ice and Climate, Niels Bohr Institute, University of Copenhagen,
Copenhagen, Denmark

Title Page

Abstract

Introduction

Conclusions

References

Tables

Figures

◀

▶

◀

▶

Back

Close

Full Screen / Esc

Printer-friendly Version

Interactive Discussion



⁹Department of Chemistry Ugo Schiff, University of Florence, Florence, Italy

¹⁰Climate and Environmental Physics, Physics Institute and Oeschger Center for Climate Change Research, University of Bern, Bern, Switzerland

Received: 14 November 2012 – Accepted: 19 November 2012

– Published: 30 November 2012

Correspondence to: L. Bazin (lucie.bazin@lsce.ipsl.fr), A. Landais (alandais@lsce.ipsl.fr)

Published by Copernicus Publications on behalf of the European Geosciences Union.

CPD

8, 5963–6009, 2012

AICC2012:
120–800 ka

L. Bazin et al.

[Title Page](#)

[Abstract](#)

[Introduction](#)

[Conclusions](#)

[References](#)

[Tables](#)

[Figures](#)

[|◀](#)

[▶|](#)

[◀](#)

[▶](#)

[Back](#)

[Close](#)

[Full Screen / Esc](#)

[Printer-friendly Version](#)

[Interactive Discussion](#)



Abstract

CPD

8, 5963–6009, 2012

An accurate and coherent chronological framework is essential for the interpretation of climatic and environmental records obtained from deep polar ice cores. Until now, one common ice core age scale has been developed based on an inverse dating method (Datice) combining glaciological modelling with absolute and stratigraphic markers between 4 ice cores covering the last 50 ka (thousand of years before present) (Lemieux-Dudon et al., 2010). In this paper, together with the companion paper of Veres et al. (2012), we present an extension of this work back to 800 ka for the NGRIP, TALDICE, EDML, Vostok and EDC ice cores using an improved version of the Datice tool. The AICC2012 (Antarctic Ice Core Chronology 2012) chronology includes numerous new gas and ice stratigraphic links as well as improved evaluation of background and associated variance scenarios. This paper concentrates on the long timescales between 120–800 ka. In this frame, new measurements of $\delta^{18}\text{O}_{\text{atm}}$ over Marine Isotope Stage (MIS) 11–12 on EDC and a complete $\delta^{18}\text{O}_{\text{atm}}$ record of the TALDICE ice cores permit us to derive new orbital gas age constraints. The coherency of the different orbitally deduced ages (from $\delta^{18}\text{O}_{\text{atm}}$, $\delta\text{O}_2/\text{N}_2$ and air content) has been verified before implementation in AICC2012. The new chronology shows only small differences, well within the original uncertainty range, when compared with the previous ice core reference age scale EDC3. For instance, the duration of the last four interglacial periods is not affected by more than 5 %. The largest deviation between AICC2012 and EDC3 (4.4 ka) is obtained around MIS 12. Despite significant modifications of the chronological constraints around MIS 5, now independent of speleothem records in AICC2012, the date of Termination II is very close to the EDC3 one.

1 Introduction

While ice core records offer a wealth of paleoclimatic and paleoenvironmental information, uncertainties associated with ice core dating limit their contribution to the

AICC2012:
120–800 ka

L. Bazin et al.

[Title Page](#)

[Abstract](#)

[Introduction](#)

[Conclusions](#)

[References](#)

[Tables](#)

[Figures](#)

◀

▶

◀

▶

[Back](#)

[Close](#)

[Full Screen / Esc](#)

[Printer-friendly Version](#)

[Interactive Discussion](#)



understanding of past climate dynamics. Age scales in calendar years have been constructed for Greenland ice cores thanks to layer counting in sites offering sufficient accumulation rates (GRIP, NGRIP) (Rasmussen et al., 2006; Svensson et al., 2006, 2008), allowing the construction of the GICC05 Greenland age scale currently spanning the past 60 ka (i.e. thousand of years before present, present being year 1950 AD in our study). Layer counting is not possible for deep Antarctic ice cores recovered in low accumulation areas and absolute time markers are generally lacking for these long Antarctic records, now extending to 800 ka. Exceptions are promising studies using $^{40}\text{Ar}/^{39}\text{Ar}$ and U/Th dating tools (Dunbar et al., 2008; Aciego et al., 2011) as well as links between ^{10}Be peaks and well dated magnetic events (Raisbeck et al., 2007) but an absolute age scale for the last 800 ka is still missing. As a result, dating of the deepest part of these Antarctic cores is largely based on various approaches combining ice flow modelling with orbital tuning.

Initial orbital dating in ice cores was inspired by orbital dating of marine cores (Imbrie and Imbrie, 1980), assuming that the Milankovitch theory (1941), linking ice volume and high latitude insolation, is correct. A similar link has been proposed between temperature records from water isotopes and the insolation curves deduced from orbital parameters (obliquity, precession) (Lorius et al., 1985). The imprint of precession in the Vostok ice core record of CH_4 concentration was also investigated (Ruddiman and Raymo, 2003). Such assumptions are however not satisfactory when one important question is to identify the insolation-climate phase relationship at orbital timescales. More recently, three different orbital dating approaches have been developed for ice core dating, independent of Antarctic climate or greenhouse gases records.

First, long records of $\delta^{18}\text{O}$ of atmospheric O_2 ($\delta^{18}\text{O}_{\text{atm}}$) have revealed that this parameter is highly correlated with insolation variations in the precession band with a lag of about 5–6 ka (Bender et al., 1994; Petit et al., 1999; Dreyfus et al., 2007). Studies have linked variations in precession to $\delta^{18}\text{O}_{\text{atm}}$ through changes in the low latitude water cycle and biospheric productivity (Bender et al., 1994; Malaizé et al., 1999; Wang et al., 2008; Severinghaus et al., 2009; Landais et al., 2007, 2010). The significant time

Title Page

Abstract

Introduction

Conclusions

References

Tables

Figures

10 of 10

Page 1

Back

Clos

Fu

-sc

Full Screen / Esc

[Printer-friendly Version](#)

Interactive Discussion



delay between changes in precession and changes in $\delta^{18}\text{O}_{\text{atm}}$ has been attributed to a combination of the 1–2 ka residence time of O_2 in the atmosphere (Bender et al., 1994; Hoffmann et al., 2004) and to the numerous and complex processes linking the isotopic composition of seawater to atmospheric oxygen via the dynamic response of the tropical water cycle to precession forcing and the associated variations in terrestrial and oceanic biospheres (Landais et al., 2010, and reference therein). This multiplicity of processes also suggests that lags may vary with time (Jouzel et al., 2002; Leuenberger, 1997). As a consequence, the $\delta^{18}\text{O}_{\text{atm}}$ record from long ice cores can be used to constrain ice core chronologies, but with a large associated uncertainty (6 ka) (Petit et al., 1999; Dreyfus et al., 2007).

Second, Bender (2002) has proposed that the elemental ratio $\delta\text{O}_2/\text{N}_2$ in the trapped air could be used as a new orbital tuning tool. Indeed, $\delta\text{O}_2/\text{N}_2$ measurements in the firn near the pore close-off depth (about 100 m below the ice-sheet surface, i.e. where unconsolidated snow is compressed and lock the air in) have revealed that the air trapping process is associated with a relative loss of O_2 with respect to N_2 (Battle et al., 1996; Severinghaus and Battle, 2006; Huber et al., 2006). Between 160 and 400 ka, the $\delta\text{O}_2/\text{N}_2$ record of the Vostok ice core displays variations similar to those of the local 21 December insolation (78° S). From these two observations, Bender (2002) formulated the hypothesis that local Antarctic summer insolation influences near-surface snow metamorphism and that this signature is preserved during the firnification process down to the pore close-off depth, where it modulates the loss of O_2 . From this hypothesis, he proposed the use of $\delta\text{O}_2/\text{N}_2$ for dating purposes and this approach was used by Kawamura et al. (2007) and Suwa and Bender (2008) to propose orbital chronologies of the Dome F and Vostok ice cores back to 360 and 400 ka, respectively. Using their high quality $\delta\text{O}_2/\text{N}_2$ record on the Dome F ice core and comparison with radiometric dating obtained on speleothem records, Kawamura et al. (2007) estimated the dating uncertainty to be as low as 0.8–2.9 ka. Still, Landais et al. (2012) have suggested that the uncertainty could be higher in some cases because (1) the tuning target is questionable and (2) the match between $\delta\text{O}_2/\text{N}_2$ and insolation signal may

[Title Page](#)[Abstract](#)[Introduction](#)[Conclusions](#)[References](#)[Tables](#)[Figures](#)[|◀](#)[▶|](#)[◀](#)[▶](#)[Back](#)[Close](#)[Full Screen / Esc](#)[Printer-friendly Version](#)[Interactive Discussion](#)

[Title Page](#)[Abstract](#)[Introduction](#)[Conclusions](#)[References](#)[Tables](#)[Figures](#)[|◀](#)[▶|](#)[◀](#)[▶](#)[Back](#)[Close](#)[Full Screen / Esc](#)[Printer-friendly Version](#)[Interactive Discussion](#)

the layer-counted Greenland GICC05 chronology over the last 6 ka, the deglaciation and the Laschamp event through 5 age constraints. Other tie points are more subject to discussion because they have underlying assumptions that some climatic events are synchronous, for example the abrupt methane increase at Termination II was assumed to be synchronous (within 2 ka) with the abrupt $\delta^{18}\text{O}$ shift in speleothem calcite recorded in the East Asia (Yuan et al., 2004) and Levantine (Bar-Matthews et al., 2003) regions at around 130.1 ka.

For ice older than the last interglacial period, tie-points were mainly derived from orbital tuning. 38 $\delta^{18}\text{O}_{\text{atm}}$ tie points with a 6 ka uncertainty were included in EDC3 between 400 and 800 ka as well as 10 air content tie points with a 4 ka uncertainty between 71 and 431 ka. The overall uncertainty attached to the EDC3 time-scale was estimated at 6 ka from 130 ka down to the bottom of the record (Parrenin et al., 2007).

The EPICA Dronning Maud Land (EDML) timescale over the past 150 ka has been derived directly from the EDC3 timescale after matching volcanic horizons between the two cores (Ruth et al., 2007). The TALos Dome ICE core (TALDICE) timescale has also been derived from other Antarctic ice cores through synchronization of the CH_4 records (Buiron et al., 2011; Schüpbach et al., 2011), CH_4 being with $\delta^{18}\text{O}_{\text{atm}}$ a global tracer of the atmosphere, hence of wide use for relative dating of ice cores (e.g. Capron et al., 2010).

Summarizing, each deep ice core has its own chronology which is not necessarily coherent with the other ice core chronologies. Typically, the Vostok GT4 and Dome C EDC3 age scales have been established separately and display significant deviations (Parrenin et al., 2007). Since some proxies are measured on the ice phase (water isotopes, dust, chemical species, ...) and other in the gas phase (CO_2 , CH_4 , ...), ice and gas age scales must be established. The ice and gas timescales are different because air is isolated from the surface at approximately 100 m under the ice-sheet surface, at the firn-ice transition, or lock-in depth (LID). In addition to the ice chronology, it is thus essential to have for each ice core a good estimate of the depth evolution of the LID to link gas and ice chronologies. According to firnification models (Herron and Langway,

[Title Page](#)[Abstract](#)[Introduction](#)[Conclusions](#)[References](#)[Tables](#)[Figures](#)[|◀](#)[▶|](#)[◀](#)[▶](#)[Back](#)[Close](#)[Full Screen / Esc](#)[Printer-friendly Version](#)[Interactive Discussion](#)

[Title Page](#)[Abstract](#)[Introduction](#)[Conclusions](#)[References](#)[Tables](#)[Figures](#)[|◀](#)[▶|](#)[◀](#)[▶](#)[Back](#)[Close](#)[Full Screen / Esc](#)[Printer-friendly Version](#)[Interactive Discussion](#)

2 Dating strategy

The Datice tool (Lemieux-Dudon et al., 2010) is a numerical program that permits to obtain the best compromise between a background chronology (based on modelling of snow accumulation rates, snow densification into ice and ice flow) and observations (absolute ages or certain reference horizons, stratigraphic links between several cores or also orbital ages).

Basically, a background scenario consists of three profiles along the ice core as a function of the depth z : the initial accumulation rate (A), the vertical thinning function (τ) and the Lock-In Depth in Ice Equivalent (LIDIE). Age scales for the ice matrix (ψ) and the gas bubbles (χ), which is assumed to be unique and the same for all species, are deduced using the following equations:

$$\psi(z) = \int_0^z \frac{D(z')}{\tau(z') \cdot A(z')} dz' \quad (1)$$

$$\Delta\text{depth}(z) \sim \text{LIDIE}(z) \cdot \tau(z) \quad (2)$$

$$\chi(z) = \psi(z - \Delta\text{depth}(z)) \quad (3)$$

where D is the relative density of the snow/ice material.

In the Datice tool, one needs to define how confident we are in the background scenarios, by determining confidence intervals (errors are assumed to be lognormal) on the accumulation, thinning and LIDIE profiles and also correlation lengths for each of these profiles (the errors in between profiles are assumed to be decorrelated). The same is true for the observations (absolute age horizons or stratigraphic links between the cores), which are assumed independent and for which a confidence interval is assigned. The Datice tool then finds the best scenario of accumulation, thinning and LIDIE and the resulting ice and gas chronologies by taking into account the background scenarios and the observations. The Datice methodology relies on the construction of a cost function, which takes into account the full dating information (background

CPD

8, 5963–6009, 2012

AICC2012:
120–800 ka

L. Bazin et al.

[Title Page](#)

[Abstract](#)

[Introduction](#)

[Conclusions](#)

[References](#)

[Tables](#)

[Figures](#)

◀

▶

◀

▶

[Back](#)

[Close](#)

[Full Screen / Esc](#)

[Printer-friendly Version](#)

[Interactive Discussion](#)



[Title Page](#)[Abstract](#)[Introduction](#)[Conclusions](#)[References](#)[Tables](#)[Figures](#)[|◀](#)[▶|](#)[◀](#)[▶](#)[Back](#)[Close](#)[Full Screen / Esc](#)[Printer-friendly Version](#)[Interactive Discussion](#)

scenarios and observations). The best scenario is the one which satisfies more closely all the dating constraints. The search of the best scenario is driven by a quasi-newton algorithm (Gilbert and Lemarechal, 1993), which requires to linearize the model equations (in order to calculate the gradient of the cost function) at each iteration.

After a revision of all the different age markers used in Lemieux-Dudon et al. (2010), we decided to remove or modify some of them: the 6 orbital tuning points due to the climatic hypothesis they are based on, the isotopic points between TALDICE and EDC, the tie-point at 130.1 ka from speleothem dating and all points derived by successive transfer from one core to another; the air content and $\delta\text{O}_2/\text{N}_2$ data are replaced by new age markers (see Sect. 3).

Few absolute ages (tephra layers, Laschamp event, Bruhnes-Matuyama reversal, layer counting) are available for the different ice cores. As a consequence, we need orbital ages ($\delta^{18}\text{O}_{\text{atm}}$, $\delta\text{O}_2/\text{N}_2$ and air content) with coherent uncertainties to constraint the timescale prior to 60 ka when layer counting is not available. We use here available $\delta^{18}\text{O}_{\text{atm}}$, $\delta\text{O}_2/\text{N}_2$ and air content profiles on the different ice cores (Dreyfus et al., 2007, 2008; Suwa and Bender, 2008; Landais et al., 2012; Raynaud et al., 2007; Lipenkov et al., 2011) completed by new $\delta^{18}\text{O}_{\text{atm}}$ data covering the period older than 50 ka on the TALDICE ice core and the period 350–450 ka on the EDC ice core.

The synchronization of the different ice cores is done through CH_4 , $\delta^{18}\text{O}_{\text{atm}}$ measurements in the gas phase (247 tie-points) and volcanic tie points in the ice phase (534 tie-points) (Udisti et al., 2004; Severi et al., 2007; Loulergue et al., 2007; Lemieux-Dudon et al., 2010; Landais et al., 2006; Loulergue, 2007; Ruth et al., 2007; Buiiron et al., 2011; Schüpbach et al., 2011; Capron et al., 2010; Schilt et al., 2010; Severi et al., 2012; Parrenin et al., 2012b; Svensson et al., 2012; Vinther et al., 2012, details in the SOM).

Additional constraints on the depth difference between a concomitant event in the ice and in the gas phases (Δdepth) are available for Greenland ice cores over the millennial scale variability of the last glacial period (Dansgaard–Oeschger events) with the use of $\delta^{15}\text{N}$ in the air trapped in the ice. Each rapid warming is indeed recorded as

[Title Page](#)[Abstract](#)[Introduction](#)[Conclusions](#)[References](#)[Tables](#)[Figures](#)[|◀](#)[▶|](#)[◀](#)[▶](#)[Back](#)[Close](#)[Full Screen / Esc](#)[Printer-friendly Version](#)[Interactive Discussion](#)

a peak in $\delta^{15}\text{N}$ (thermal isotopic fractionation) in the gas phase and as a step in the ice $\delta^{18}\text{O}$. The depth difference between the $\delta^{15}\text{N}$ peak and the ice $\delta^{18}\text{O}$ step has been measured for DO 9–25 on the NorthGRIP ice core (Landais et al., 2004, 2005; Huber et al., 2006; Capron et al., 2010) defining 15 constraints for the Δ depth (table in SOM).

- Finally, it has been suggested that $\delta^{15}\text{N}$ in Antarctica can also be used for improving our estimate of LID independently of firnification models (Parrenin et al., 2012a). This is based on the assumption that the firn depth, from surface to the LID, is always equal to the depth of the diffusive zone, which can be inferred from $\delta^{15}\text{N}$ data. While this is very often the case for present day firns (Landais et al., 2006), a convective zone of about 20 m may exist during glacial period in remote sites of East Antarctica (Severinghaus et al., 2010). We thus refrain from imposing any delta-depth constraints from $\delta^{15}\text{N}$ profiles in Antarctica but use these data for the LIDIE background scenario (details in SOM).

3 Orbital markers

- As discussed above, the most critical aspect for the 120–800 ka dating is the availability and use of the orbital markers. In a first sub-section, we will provide new $\delta^{18}\text{O}_{\text{atm}}$ data for orbital constraints on TALDICE and EDC. In a second sub-section, we review and evaluate dating uncertainties of the available $\delta^{18}\text{O}_{\text{atm}}$, $\delta\text{O}_2/\text{N}_2$ and air content series.

3.1 New measurements

- All measurements of $\delta^{18}\text{O}_{\text{atm}}$ of air trapped in the ice cores of EDC and TALDICE were performed at LSCE, using a melt-refreeze method (Sowers et al., 1989; Landais et al., 2003a). The analyses were conducted on a Delta V plus (thermo Electron Corporation) mass spectrometer and data were corrected for mass interferences (Severinghaus et al., 2001; Landais et al., 2003a). The measurements were calibrated against current dried exterior air. The $\delta^{18}\text{O}_{\text{atm}}$ is obtained after correction of the $\delta^{18}\text{O}$ of O_2 for

[Title Page](#)[Abstract](#)[Introduction](#)[Conclusions](#)[References](#)[Tables](#)[Figures](#)[|◀](#)[▶|](#)[◀](#)[▶](#)[Back](#)[Close](#)[Full Screen / Esc](#)[Printer-friendly Version](#)[Interactive Discussion](#)

the gravitational isotopic fractionation in the firn ($\delta^{18}\text{O}_{\text{atm}} = \delta^{18}\text{O} - 2\delta^{15}\text{N}$). The resulting data set has a precision of roughly 0.03 ‰ (1 sigma uncertainty).

3.1.1 $\delta^{18}\text{O}_{\text{atm}}$ of EDC

The first EDC $\delta^{18}\text{O}_{\text{atm}}$ record has been produced by Dreyfus et al. (2007, 2008) between 300 and 800 ka with a mean resolution of 1.5 ka. They defined 38 tie-points by aligning mid-slope variations of $\delta^{18}\text{O}_{\text{atm}}$ with their counterparts in the precession parameter (delayed by 5 ka), leading to an uncertainty of 6 ka for each tie-point. Still, the period covering 300–410 ka and including MIS 11 shows $\delta^{18}\text{O}_{\text{atm}}$ variations that cannot unambiguously match the precession curve (Fig. 1). This is probably due to the low eccentricity damping of the precession variations at that period. As a consequence, the 6 tie-points originally proposed over this period can be challenged.

We have performed $\delta^{18}\text{O}_{\text{atm}}$ measurements on 92 new ice samples from EDC between 2479 and 2842 m (covering 300 to 500 ka) with a mean resolution of 1 ka.

With our improved resolution of the $\delta^{18}\text{O}_{\text{atm}}$ signal over this period, we are now able to better constrain the EDC chronology by orbital tuning. To do so, we strictly follow the methodology of Dreyfus et al. (2007) described above. We obtain 7 new orbital tuned ages for the gas phase of EDC ice core, replacing the first 6 points of the Table 1 of Dreyfus et al. (2007). Finally, we end up with 39 $\delta^{18}\text{O}_{\text{atm}}$ points to be used as orbital constraints in the gas phase for the EDC ice core (Table 1).

3.1.2 $\delta^{18}\text{O}_{\text{atm}}$ of TALDICE

Burion et al. (2011) have measured the $\delta^{18}\text{O}_{\text{atm}}$ of TALDICE between 583 m and 1402 m (9.4 ka and 125.8 ka) and could identify clear precession driven $\delta^{18}\text{O}_{\text{atm}}$ cycles around 10 and 85 ka. However significant gaps remained at 24–33 ka, 81–110 ka and before 126 ka. With now 83 new depth levels measured in this study, we obtain a complete record of $\delta^{18}\text{O}_{\text{atm}}$ along the entire core with a mean resolution of 1.5 ka (Fig. 2).

Using the original TALDICE 1a age scale (Buiron et al., 2011; Schüpbach et al., 2011), the full $\delta^{18}\text{O}_{\text{atm}}$ record displays clear ~ 23 ka cycles corresponding to precession variations back to 200 ka (Fig. 2). Prior to 200 ka, $\delta^{18}\text{O}_{\text{atm}}$ shows a large variability with much higher frequency variations. This questions the integrity of the record. Spurious variations of $\delta^{18}\text{O}_{\text{atm}}$ can indeed be used, together with methane, to check the integrity of ice core records especially on their bottom part by comparison with undisturbed records of the same time period (Landais et al., 2003b). A comparison of the methane and $\delta^{18}\text{O}_{\text{atm}}$ records of Vostok and TALDICE ice cores over the last 300 ka on their respective chronologies (Fig. 3) shows significant differences. Over the last 150 ka, differences are most probably due to the different age scales of the ice cores since the CH_4 and $\delta^{18}\text{O}_{\text{atm}}$ sequences and amplitudes are similar despite small shifts between the two ice cores. Prior to 150 ka, the methane record has a poor resolution and the two $\delta^{18}\text{O}_{\text{atm}}$ records show significant differences in amplitude and frequency before 200 ka. We have thus decided to stop analysis and chronologies at 150 ka (corresponding to ~ 1500 m depth) for the TALDICE ice core until new methane and $\delta^{18}\text{O}_{\text{atm}}$ measurements are performed allowing to assess the integrity of the stratigraphy. Note that surprisingly large ice crystals have been observed below 1500 m on the TALDICE ice core, which further questions the integrity of the core.

Using TALDICE $\delta^{18}\text{O}_{\text{atm}}$ back to 150 ka and applying the same method described for EDC, we determine 8 orbital gas ages by tuning on the precession parameter delayed by 5 ka (Table 2).

3.2 Orbital points database

In this section, we combine the new orbital tie-points derived in the previous section and the orbital tie points already available from previous studies.

CPD

8, 5963–6009, 2012

AICC2012:
120–800 ka

L. Bazin et al.

[Title Page](#)

[Abstract](#)

[Introduction](#)

[Conclusions](#)

[References](#)

[Tables](#)

[Figures](#)

◀

▶

◀

▶

[Back](#)

[Close](#)

[Full Screen / Esc](#)

[Printer-friendly Version](#)

[Interactive Discussion](#)



3.2.1 $\delta^{18}\text{O}_{\text{atm}}$

CPD

8, 5963–6009, 2012

AICC2012:
120–800 ka

L. Bazin et al.

In addition to the EDC and TALDICE $\delta^{18}\text{O}_{\text{atm}}$ markers discussed above, we also use the markers deduced by Suwa and Bender (2008) for Vostok (Table 2 therein). The tuning is slightly different than the one chosen by Dreyfus et al. (2007) (tuning on the 5 65° N June insolation curve with a delay of 5.9 ka instead of tuning on the precession signal with a 5 ka delay). A comparison of both tuning strategies has shown that they are equivalent (Dreyfus et al., 2007).

Altogether, we now have a database of $\delta^{18}\text{O}_{\text{atm}}$ with 39 gas age markers for EDC, 8 for TALDICE and 35 for Vostok. The uncertainty associated with all these points is estimated to be a quarter of a precession period (Dreyfus et al., 2007), leading to a value of 6 ka. This relatively large uncertainty accounts for the uncertainty in the choice of the orbital target and for the fact that the shift between $\delta^{18}\text{O}_{\text{atm}}$ and precession is known to vary with time, especially over terminations (Jouzel et al., 2002; Kawamura et al., 2007).

3.2.2 $\delta\text{O}_2/\text{N}_2$

For the aim of the AICC2012 chronology, two $\delta\text{O}_2/\text{N}_2$ records are available: Vostok (100–400 ka, Suwa and Bender, 2008) and EDC (300 to 800 ka, Landais et al., 2012). While Suwa and Bender (2008) already produced 27 $\delta\text{O}_2/\text{N}_2$ orbital tie-points using as target the local December insolation, no tie-points were proposed by Landais et al. (2012). Here, we have derived 20 orbital ages from the EDC $\delta\text{O}_2/\text{N}_2$ record (Table 3). To do this, the $\delta\text{O}_2/\text{N}_2$ signal is filtered with a band pass between $1/15\text{ ka}^{-1}$ and $1/100\text{ ka}^{-1}$. Its mid slope variations are then associated with the mid-slopes of the local summer solstice insolation signal. No tie-points were attributed in periods with too low $\delta\text{O}_2/\text{N}_2$ resolution and in periods without a clear correspondence between the $\delta\text{O}_2/\text{N}_2$ record and the insolation curve.

[Title Page](#)

[Abstract](#)

[Introduction](#)

[Conclusions](#)

[References](#)

[Tables](#)

[Figures](#)

◀

▶

◀

▶

[Back](#)

[Close](#)

[Full Screen / Esc](#)

[Printer-friendly Version](#)

[Interactive Discussion](#)



We have decided to attribute a conservative uncertainty of 4 ka to all of these tie points (both for Vostok and EDC) because of the low quality of the measurements (gas loss) and questions about the phasing of local insolation curve and $\delta\text{O}_2/\text{N}_2$ curve (Landais et al., 2012).

5 3.2.3 Air content

Air content measurements have been published for the Vostok ice core (150–400 ka, Lipenkov et al., 2011) and for the youngest part of the EDC ice core (0–440 ka, Raynaud et al., 2007) but no orbital tie-points were provided. To build such tables, we have followed two different approaches, the one proposed by Raynaud et al. (2007) and the 10 one similar to what has been applied for $\delta\text{O}_2/\text{N}_2$ and $\delta^{18}\text{O}_{\text{atm}}$.

The method used by Raynaud et al. (2007) and Lipenkov et al. (2011) is to calculate the time delay between air content, filtered in the $1/15\text{ ka}^{-1}$ and $1/46\text{ ka}^{-1}$ pass-band, and the integrated local summer insolation (ISI). The ISI curve is obtained by summation of all daily summer insolation above a certain threshold; the threshold being inferred such that the ISI curve has the same spectral properties as the air content. With the resulting time delay it is possible to associate orbital ages with the mid-slope variations of the air content. Using this method, we have determined 14 and 8 orbital ice ages for EDC and Vostok ice cores respectively (Tables 4 and 5). In order to verify the robustness of these points, we also deduced ages by direct matching of the mid-slope variations of the unfiltered air content with the mid-slopes of the ISI target. All 15 ages obtained are consistent within ± 1 ka on average. The uncertainty for each point was calculated as a function of the sampling resolution, the uncertainty of the currently used chronology, the uncertainty of the ISI curves and the age difference with the direct 20 mid-slope method, leading to values from 2.9 ka to 7.2 ka.

CPD

8, 5963–6009, 2012

AICC2012:
120–800 ka

L. Bazin et al.

[Title Page](#)

[Abstract](#)

[Introduction](#)

[Conclusions](#)

[References](#)

[Tables](#)

[Figures](#)

◀

▶

◀

▶

[Back](#)

[Close](#)

[Full Screen / Esc](#)

[Printer-friendly Version](#)

[Interactive Discussion](#)



3.3 Coherency of orbital markers for the Vostok ice core

AICC2012:
120–800 ka

L. Bazin et al.

[Title Page](#)

[Abstract](#)

[Introduction](#)

[Conclusions](#)

[References](#)

[Tables](#)

[Figures](#)

◀

▶

◀

▶

[Back](#)

[Close](#)

[Full Screen / Esc](#)

[Printer-friendly Version](#)

[Interactive Discussion](#)



[Title Page](#)[Abstract](#)[Introduction](#)[Conclusions](#)[References](#)[Tables](#)[Figures](#)[|◀](#)[▶|](#)[◀](#)[▶](#)[Back](#)[Close](#)[Full Screen / Esc](#)[Printer-friendly Version](#)[Interactive Discussion](#)

- incorrect Δ age or LIDIE estimates, since the $\delta\text{O}_2/\text{N}_2$ and air content markers are ice age markers and the $\delta^{18}\text{O}_{\text{atm}}$ is a gas age constraint;
- incorrect orbital targets for $\delta\text{O}_2/\text{N}_2$, air content and $\delta^{18}\text{O}_{\text{atm}}$. In particular, no definitive quantitative explanation has been given for the 5 ka lag between precession parameter and $\delta^{18}\text{O}_{\text{atm}}$. Similarly, it is still under discussion if the $\delta\text{O}_2/\text{N}_2$ curve should be strictly aligned with the summer solstice insolation (Landais et al., 2012; Hutterli et al., 2010).

Moreover, for each orbital tuning, lags between the records and their orbital targets may vary with time (Jouzel et al., 2002).

- We conclude that all orbitally tuned chronologies agree well one with each other. This permits us to safely combine the ice and gas orbital ages within their uncertainty range.

4 New chronology

4.1 Chronology construction

- When combining all the different observations (absolute ages, stratigraphic links, Δ depth and orbital ages), 7 orbital markers have been removed because they led to abrupt variations in the thinning function or anomalous peaks of LIDIE, which are not realistic (see SOM). The removed points are indicated by a “*” in Tables 1 and 3: 4 ice age markers from $\delta\text{O}_2/\text{N}_2$ and 3 gas age markers from $\delta^{18}\text{O}_{\text{atm}}$ of the EDC ice core. After comparing their position with the eccentricity curve, it appears that 5 of these points (3 $\delta^{18}\text{O}_{\text{atm}}$ and 2 $\delta\text{O}_2/\text{N}_2$) are located near eccentricity minima (438 ka and 534 ka). For the last two points of $\delta\text{O}_2/\text{N}_2$, they are again located during a minimum of eccentricity period (750–815 ka) and are conflicting with the absolute age of the Bruhnes-Matuyama reversal.

300 different Datice simulations were run to optimize the final AICC2012 chronology. In addition to tests of the coherency for the different absolute, orbital and stratigraphic points, it has been found that the background parameters and associated variances have a strong influence on the final chronologies. For example, we had to strongly enlarge the variance of the TALDICE thinning function. Indeed, the background chronology of TALDICE has a much too young Termination II (110 ka), which is unrealistic and should not influence the final AICC2012 chronology.

4.2 The new AICC2012 chronology on orbital timescale

As expected from the numerous stratigraphic markers distributed on the 5 ice cores, the variations imprinted in the methane and isotopic composition are synchronous within 1.5 ka for our five ice cores on the new AICC2012 chronology over the last 350 ka (Fig. 5). Prior to 350 ka, there is no stratigraphic tie-point between EDC and Vostok so that the AICC2012 chronologies are independently established for Vostok and EDC, using their individual $\delta^{18}\text{O}_{\text{atm}}$, $\delta\text{O}_2/\text{N}_2$ and air content markers indicated on Fig. 5. New measurements of CH_4 and $\delta^{18}\text{O}_{\text{atm}}$ are strongly needed to provide stratigraphic links between the two cores back to 400 ka.

The new AICC2012 chronology is in rather good agreement (within 2–3 ka) with the previous EDC3 timescale (Parrenin et al., 2007) when comparing the water isotope and CH_4 records of EDC (Fig. 6). In particular, it does not modify significantly the length of interglacial periods (Table 6). Nevertheless, one period shows significant differences, up to 4.4 ka (shaded zone on Fig. 6), corresponding to MIS 12. Termination V appears similar (within 330 a) in AICC2012 and EDC3, and MIS 11 duration is not significantly changed (Table 6). This period is close to the minimum of eccentricity characterizing MIS 11, which makes the identification of orbital markers difficult by comparison of $\delta\text{O}_2/\text{N}_2$ and $\delta^{18}\text{O}_{\text{atm}}$ records with their respective tuning targets. In this study we have improved the resolution of EDC $\delta^{18}\text{O}_{\text{atm}}$ over MIS 11–12, leading to the determination of new orbital ages replacing those of Dreyfus et al. (2007), used to construct the EDC3

[Title Page](#)[Abstract](#)[Introduction](#)[Conclusions](#)[References](#)[Tables](#)[Figures](#)[|◀](#)[▶|](#)[◀](#)[▶](#)[Back](#)[Close](#)[Full Screen / Esc](#)[Printer-friendly Version](#)[Interactive Discussion](#)

chronology. Consequently, the differences observed over this period between the two chronologies mainly result from the replacement of the $\delta^{18}\text{O}_{\text{atm}}$ age markers and the addition of ice age markers. Because the identification of orbital age markers is difficult over this period of low eccentricity, new measurements of $\delta\text{O}_2/\text{N}_2$ and air content on the EDC ice core are still needed especially for the small precession peaks at 350–450 ka.

The dating improvements for the AICC2012 chronology concern mainly the last 150 ka where the numerous new stratigraphic links permit to significantly decrease the dating uncertainties. In the companion paper, Veres et al. (2012) mainly discuss the millennial scale variability of the last 120 ka and we focus here on MIS 5.5. The records are coherent over this period between the 4 Antarctic ice cores (Fig. 7), within the uncertainty of AICC2012, with the Vostok ice core being slightly older (1 ka) than the other ice cores. The duration of MIS 5.5, defined here by the $-403\text{\textperthousand}$ threshold of δD on EDC (EPICA Community Members, 2004), is slightly longer in AICC2012 (16.9 ka) compared to its duration in the EDC3 chronology (16.2 ka) and the age of Termination II is not significantly modified compared to its age in EDC3. Still, the reduction of uncertainty associated with the age of Termination II and MIS 5.5 compared to previous ice core chronologies makes it interesting to compare our result with other dated records.

Absolute dating of Termination II has been possible in at least two well-dated speleothems. In China, Cheng et al. (2009) dated a strong decrease of calcite $\delta^{18}\text{O}$ in the Sanbao cave speleothem at 128.91 ± 0.06 ka. In Italy, Drysdale et al. (2009) obtained a decrease in calcite $\delta^{18}\text{O}$ on a speleothem of the Corchia cave in two steps: a first $1.5\text{\textperthousand}$ decrease between 133 and 131 ka and a second decrease of 1\textperthousand between 129 and 128 ka. There is a priori no contradiction between these two dates since calcite $\delta^{18}\text{O}$ reflects local or regional intensity of the hydrological cycle in China while the impact of local temperature on meteoric water and then calcite $\delta^{18}\text{O}$ is expected to be more pronounced in Italy. The different dates for the calcite $\delta^{18}\text{O}$ decrease may thus reflect different regional climatic response during Termination II.

[Title Page](#)[Abstract](#)[Introduction](#)[Conclusions](#)[References](#)[Tables](#)[Figures](#)[|◀](#)[▶|](#)[◀](#)[▶](#)[Back](#)[Close](#)[Full Screen / Esc](#)[Printer-friendly Version](#)[Interactive Discussion](#)

[Title Page](#)[Abstract](#)[Introduction](#)[Conclusions](#)[References](#)[Tables](#)[Figures](#)[|◀](#)[▶|](#)[◀](#)[▶](#)[Back](#)[Close](#)[Full Screen / Esc](#)[Printer-friendly Version](#)[Interactive Discussion](#)

[Title Page](#)[Abstract](#)[Introduction](#)[Conclusions](#)[References](#)[Tables](#)[Figures](#)[|◀](#)[▶|](#)[◀](#)[▶](#)[Back](#)[Close](#)[Full Screen / Esc](#)[Printer-friendly Version](#)[Interactive Discussion](#)

difficult at that time. New measurements on well-conserved ice should be performed to improve the records.

Finally, the AICC2012 chronology suggests synchronous millennial variations of water stable isotopes at EDC, EDML, and Vostok during the last interglacial, supporting earlier hypotheses (Masson-Delmotte et al., 2011). It also highlights a sharp cooling at 117 ka synchronous in EDML and TALDICE, and distinct from the other more inland records. This behavior is inferred from the stratigraphic links between the Antarctic ice cores and also the $\delta^{18}\text{O}_{\text{atm}}$ markers of TALDICE around this period. It confirms the different isotope trend at TALDICE and EDC during the last interglacial period, supporting interpretations of this gradient as a glaciological fingerprint of changes in East Antarctic ice sheet topography (Bradley et al., 2012).

5 Conclusions

In this study, together with the companion study of Veres et al. (2012), we have established a new reference chronology for 4 Antarctic ice cores, AICC2012 covering the last 800 ka. An important aspect of the common chronology development has been the compilation of absolute and stratigraphic tie-points as well as a careful evaluation of the background scenarios and associated variances for thinning, accumulation rate and LIDIE. These results are available in the supplementary material associated with the AICC2012 chronology.

More specifically, we have focused here on the orbital timescale between 120 and 800 ka. First, we have presented new measurements of $\delta^{18}\text{O}_{\text{atm}}$ of EDC over MIS 11–12 to improve the determination of orbital markers over this period characterized by a low eccentricity. Second, we have provided a complete record of $\delta^{18}\text{O}_{\text{atm}}$ for the TALDICE ice core prior to 50 ka. This new record has permitted to provide 8 new orbital markers over the last 150 ka of the TALDICE ice core. With this new record, we have also pointed out that the integrity of the ice core prior to 150 ka is questionable. Third, we have tested the coherency of the different orbital ages derived from air content,

[Title Page](#)[Abstract](#)[Introduction](#)[Conclusions](#)[References](#)[Tables](#)[Figures](#)[|◀](#)[▶|](#)[◀](#)[▶](#)[Back](#)[Close](#)[Full Screen / Esc](#)[Printer-friendly Version](#)[Interactive Discussion](#)

in Greenland, all of these ice cores being highly documented with absolute or orbital markers.

CPD

8, 5963–6009, 2012

**Supplementary material related to this article is available online at:
<http://www.clim-past-discuss.net/8/5963/2012/cpd-8-5963-2012-supplement.pdf>.**

5

AICC2012:
120–800 ka

L. Bazin et al.

Acknowledgements. We thank the EDC4 team for stimulating the discussion around the building of AICC2012 and helping to pick up the best parameters to feed the Datice tool. This project was funded by the “Fondation de France Ars Cuttoli”, INRIA and LEFE funding. It was also supported by the Past4Future project of the European Commission’s 7th Framework Programme under Grant agreement no. 243908. It is a contribution to the European Project for Ice Coring in Antarctica (EPICA), a joint European Science Foundation/European Commission scientific programme, funded by the EU and by national contributions from Belgium, Denmark, France, Germany, Italy, the Netherlands, Norway, Sweden, Switzerland and the UK. The main logistic support was provided by IPEV and PNRA (at Dome C) and AWI (at Dronning Maud Land). This is an EPICA publication no. XXX. This is Past4Future contribution number XXX. This is LSCE contribution no. XXX. We address special thanks to Sébastien Nomade and Frédéric Prié for their help in this study.



20 The publication of this article is financed by CNRS-INSU.

Discussion Paper | Discussion Paper | Discussion Paper | Discussion Paper

Title Page

Abstract

Introduction

Conclusions

References

Tables

Figures

◀

▶

◀

▶

Back

Close

Full Screen / Esc

Printer-friendly Version

Interactive Discussion



References

AICC2012:
120–800 ka

L. Bazin et al.

- Aciego, S., Bourdon, B., Schwander, J., Baur, H., and Forieri, A.: Toward a radiometric ice clock: uranium ages of the Dome C ice core, *Quaternary Sci. Rev.*, 30, 2389–2397, doi:10.1016/j.quascirev.2011.06.008, 2011. 5966
- 5 Arnaud, L., Barnola, J.-M., and Duval, P.: Physical modeling of the densification of snow/firn and ice in the upper part of polar ice sheets, Book: *Physics of Ice Core Records*, 285–305, edited by: Hondoh, T., Hokkaido Univ. Press, Sapporo, Japan, 2000 5970
- 10 Bar-Matthews, M., Ayalon, A., Gilmour, M., Matthews, A., and Hawkesworth, C. J.: Sea-land oxygen isotopic relationships from planktonic foraminifera and speleothems in the Eastern Mediterranean region and their implication for paleorainfall during interglacial intervals, *Geochim. Cosmochim. Ac.*, 67, 3181–3199, doi:10.1016/S0016-7037(02)01031-1, 2003. 5969
- 15 Battle, M., Bender, M., Sowers, T., Tans, P. P., Butler, J. H., Elkins, J. W., Ellis, J. T., Conway, T., Zhang, N., Lang, P., and Clarket, A. D.: Atmospheric gas concentrations over the past century measured in air from firn at the South Pole, *Nature*, 383, 231–235, doi:10.1038/383231a0, 1996. 5967
- 20 Bender, M. L.: Orbital tuning chronology for the Vostok climate record supported by trapped gas composition, *Earth Planet. Sci. Lett.*, 204, 275–289, doi:10.1016/S0012-821X(02)00980-9, 2002. 5967, 6005
- 25 Bender, M., Sowers, T., and Labeyrie, L.: The Dole effect and its variations during the last 130 000 years as measured in the Vostok ice core, *Global Biogeochem. Cy.*, 8, 363–376, doi:10.1029/94GB00724, 1994. 5966, 5967
- Bradley, S. L., Siddall, M., Milne, G. A., Masson-Delmotte, V., and Wolff, E.: Combining ice core records and ice sheet models to explore the evolution of the East Antarctic Ice sheet during the Last Interglacial period, *Global Planet. Change*, accepted, 2012. 5983
- 30 Buiiron, D., Chappellaz, J., Stenni, B., Frezzotti, M., Baumgartner, M., Capron, E., Landais, A., Lemieux-Dudon, B., Masson-Delmotte, V., Montagnat, M., Parrenin, F., and Schilt, A.: TALDICE-1 age scale of the Talos Dome deep ice core, East Antarctica, *Clim. Past*, 7, 1–16, doi:10.5194/cp-7-1-2011, 2011. 5969, 5972, 5974, 5975, 6004, 6005, 6007
- Caillon, N., Severinghaus, J. P., Jouzel, J., Barnola, J.-M., Kang, J., and Lipenkov, V. Y.: Timing of atmospheric CO₂ and Antarctic temperature changes across termination III, *Science*, 299, 1728–1731, doi:10.1126/science.1078758, 2003. 6005, 6007

Title Page

Abstract

Introduction

Conclusions

References

Tables

Figures

◀

▶

◀

▶

Back

Close

Full Screen / Esc

Printer-friendly Version

Interactive Discussion



Capron, E., Landais, A., Lemieux-Dudon, B., Schilt, A., Masson-Delmotte, V., Buiron, D., Chappellaz, J., Dahl-Jensen, D., Johnsen, S., Leuenberger, M., Loulergue, L., and Oerter, H.: Synchronising EDML and NorthGRIP ice cores using $\delta^{18}\text{O}$ of atmospheric oxygen ($\delta^{18}\text{O}_{\text{atm}}$) and CH_4 measurements over MIS5 (80–123 kyr), *Quaternary Sci. Rev.*, 29, 222–234, 5 doi:10.1016/j.quascirev.2009.07.014, 2010. 5969, 5972, 5973, 6007

Capron, E., Landais, A., Buiron, D., Cauquoin, A., Chappellaz, J., Debret, M., Jouzel, J., Leuenberger, M., Martinerie, P., Masson-Delmotte, V., Mulvaney, R., Parrenin, F., and Prié, F.: Glacial-interglacial dynamics of Antarctic firns: comparison between simulations and ice core air-d15N measurements, *Clim. Past*, this issue, in preparation, 2012. 5970, 5984

Cheng, H., Edwards, R. L., Broecker, W. S., Denton, G. H., Kong, X., Wang, Y., Zhang, R., and Wang, X.: Ice Age terminations, *Science*, 326, 248–252, doi:10.1126/science.1177840, 10 2009. 5981

Delmotte, M., Chappellaz, J., Brook, E., Yiou, P., Barnola, J. M., Goujon, C., Raynaud, D., and Lipenkov, V. I.: Atmospheric methane during the last four glacial-interglacial cycles: rapid changes and their link with Antarctic temperature, *J. Geophys. Res.-Atmos.*, 109, D12104, 15 doi:10.1029/2003JD004417, 2004. 6005, 6007

Dreyfus, G. B., Parrenin, F., Lemieux-Dudon, B., Durand, G., Masson-Delmotte, V., Jouzel, J., Barnola, J.-M., Panno, L., Spahni, R., Tisserand, A., Siegenthaler, U., and Leuenberger, M.: Anomalous flow below 2700 m in the EPICA Dome C ice core detected using $\delta^{18}\text{O}$ of atmospheric oxygen measurements, *Clim. Past*, 3, 341–353, doi:10.5194/cp-3-341-2007, 2007. 20 5966, 5967, 5972, 5974, 5976, 5980, 5997, 6003

Dreyfus, G. B., Raisbeck, G. M., Parrenin, F., Jouzel, J., Guyodo, Y., Nomade, S., and Mazaad, A.: An ice core perspective on the age of the Matuyama–Brunhes boundary, *Earth Planet. Sci. Lett.*, 274, 151–156, doi:10.1016/j.epsl.2008.07.008, 2008. 5972, 5974, 6003

Drysdale, R. N., Hellstrom, J. C., Zanchetta, G., Fallick, A. E., Sanchez Goñi, M. F., Couichoud, I., McDonald, J., Maas, R., Lohmann, G., and Isola, I.: Evidence for obliquity forcing of glacial termination II, *Science*, 325, 1527–1531, doi:10.1126/science.1170371, 2009. 25 5981

Dunbar, N. W., McIntosh, W. C., and Esser, R. P.: Physical setting and tephrochronology of the summit caldera ice record at Mount Moulton, West Antarctica, *Geol. Soc. Am. Bull.*, 120, 796–812, doi:10.1130/B26140.1, 2008. 5966, 5968

EPICA Community Members: Eight glacial cycles from an Antarctic ice core, *Nature*, 429, 623–628, doi:10.1038/nature02599, 2004. 5981, 6008

CPD

8, 5963–6009, 2012

AICC2012:
120–800 ka

L. Bazin et al.

[Title Page](#)

[Abstract](#)

[Introduction](#)

[Conclusions](#)

[References](#)

[Tables](#)

[Figures](#)

[|◀](#)

[▶|](#)

[◀](#)

[▶](#)

[Back](#)

[Close](#)

[Full Screen / Esc](#)

[Printer-friendly Version](#)

[Interactive Discussion](#)



AICC2012:
120–800 ka

L. Bazin et al.

[Title Page](#)[Abstract](#)[Introduction](#)[Conclusions](#)[References](#)[Tables](#)[Figures](#)[◀](#)[▶](#)[◀](#)[▶](#)[Back](#)[Close](#)[Full Screen / Esc](#)[Printer-friendly Version](#)[Interactive Discussion](#)

Hutterli, M. A., Schneebeli, M., Freitag, J., Kipfstuhl, J., and Rothlisberger, R.: Impact of local insolation on snow metamorphism and ice core records, in: Physics of Ice Core Records II, edited by: Honda, T., Hokkaido University Press, 223–232, Sapporo, Japan, 2010. 5979

Imbrie, J. and Imbrie, J. Z.: Modeling the climatic response to orbital variations, *Science*, 207, 943–953, doi:10.1126/science.207.4434.943, 1980. 5966

Jouzel, J., Hoffmann, G., Parrenin, F., and Waelbroeck, C.: Atmospheric oxygen 18 and sea-level changes, *Quaternary Sci. Rev.*, 21, 307–314, doi:10.1016/S0277-3791(01)00106-8, 2002. 5967, 5976, 5979

Jouzel, J., Masson-Delmotte, V., Cattani, O., Dreyfus, G., Falourd, S., Hoffmann, G., Miner, B., Nouet, J., Barnola, J. M., Chappellaz, J., Fischer, H., Gallet, J. C., Johnsen, S., Leuenberger, M., Louergue, L., Luethi, D., Oerter, H., Parrenin, F., Raisbeck, G., Raynaud, D., Schilt, A., Schwander, J., Selmo, E., Souchez, R., Spahni, R., Stauffer, B., Steffensen, J. P., Stenni, B., Stocker, T. F., Tison, J. L., Werner, M., and Wolff, E. W.: Orbital and millennial Antarctic climate variability over the past 800 000 Years, *Science*, 317, 793–796, doi:10.1126/science.1141038, 2007. 5968, 5984, 6003, 6007

Kawamura, K., Parrenin, F., Lisiecki, L., Uemura, R., Vimeux, F., Severinghaus, J. P., Hutterli, M. A., Nakazawa, T., Aoki, S., Jouzel, J., Raymo, M. E., Matsumoto, K., Nakata, H., Motoyama, H., Fujita, S., Goto-Azuma, K., Fujii, Y., and Watanabe, O.: Northern Hemisphere forcing of climatic cycles in Antarctica over the past 360 000 years, *Nature*, 448, 912–916, doi:10.1038/nature06015, 2007. 5967, 5976, 5982, 6009

Landais, A., Caillon, N., Severinghaus, J., Jouzel, J., and Masson-Delmotte, V.: Analyses isotopiques à haute précision de l'air piégé dans les glaces polaires pour la quantification des variations rapides de température: méthodes et limites, Notes des activités instrumentales de l'IPSL, Technical Report, 39, 2003a. 5973

Landais, A., Chappellaz, J., Delmotte, M., Jouzel, J., Blunier, T., Bourg, C., Caillon, N., Charrer, S., Malaizé, B., Masson-Delmotte, V., Raynaud, D., Schwander, J., and Steffensen, J. P.: A tentative reconstruction of the last interglacial and glacial inception in Greenland based on new gas measurements in the Greenland Ice Core Project (GRIP) ice core, *J. Geophys. Res.-Atmos.*, 108, 4563, doi:10.1029/2002JD003147, 2003b. 5975

Landais, A., Barnola, J. M., Masson-Delmotte, V., Jouzel, J., Chappellaz, J., Caillon, N., Huber, C., Leuenberger, M., and Johnsen, S. J.: A continuous record of temperature evolution over a sequence of Dansgaard-Oeschger events during Marine Isotopic Stage 4 (76 to 62 kyr BP), *Geophys. Res. Lett.*, 31, L22211, doi:10.1029/2004GL021193, 2004. 5973

[Title Page](#)[Abstract](#)[Introduction](#)[Conclusions](#)[References](#)[Tables](#)[Figures](#)[◀](#)[▶](#)[◀](#)[▶](#)[Back](#)[Close](#)[Full Screen / Esc](#)[Printer-friendly Version](#)[Interactive Discussion](#)

Landais, A., Jouzel, J., Massondelmotte, V., and Caillon, N.: Large temperature variations over rapid climatic events in Greenland: a method based on air isotopic measurements, *C. R. Geosci.*, 337, 947–956, doi:10.1016/j.crte.2005.04.003, 2005. 5973

Landais, A., Waelbroeck, C., and Masson-Delmotte, V.: On the limits of Antarctic and marine climate records synchronization: lag estimates during marine isotopic stages 5d and 5c, *Paleoceanography*, 21, PA1001, doi:10.1029/2005PA001171, 2006. 5972, 5973

Landais, A., Masson-Delmotte, V., Combourieu Nebout, N., Jouzel, J., Blunier, T., Leuenberger, M., Dahl-Jensen, D., and Johnsen, S.: Millennial scale variations of the isotopic composition of atmospheric oxygen over Marine Isotopic Stage 4, *Earth Planet. Sci. Lett.*, 258, 101–113, doi:10.1016/j.epsl.2007.03.027, 2007. 5966

Landais, A., Dreyfus, G., Capron, E., Masson-Delmotte, V., Sanchez-Goñi, M., Desprat, S., Hoffmann, G., Jouzel, J., Leuenberger, M., and Johnsen, S.: What drives the millennial and orbital variations of $\delta^{18}\text{O}_{\text{atm}}$?, *Quat. Sci. Rev.*, 29, 235–246, doi:10.1016/j.quascirev.2009.07.005, 2010. 5966, 5967

Landais, A., Dreyfus, G., Capron, E., Pol, K., Loutre, M. F., Raynaud, D., Lipenkov, V. Y., Arnaud, L., Masson-Delmotte, V., Paillard, D., Jouzel, J., and Leuenberger, M.: Towards orbital dating of the EPICA Dome C ice core using $\delta\text{O}_2/\text{N}_2$, *Clim. Past*, 8, 191–203, doi:10.5194/cp-8-191-2012, 2012. 5967, 5972, 5976, 5977, 5979, 5999

Laskar, J., Robutel, P., Joutel, F., Gastineau, M., Correia, A. C. M., and Levrard, B.: A long-term numerical solution for the insolation quantities of the Earth, *Astron. Astrophys.*, 428, 261–285, doi:10.1051/0004-6361:20041335, 2004. 6003

Lemieux-Dudon, B., Blayo, E., Petit, J.-R., Waelbroeck, C., Svensson, A., Ritz, C., Barnola, J.-M., Narcisi, B. M., and Parrenin, F.: Consistent dating for Antarctic and Greenland ice cores, *Quat. Sci. Rev.*, 29, 8–20, doi:10.1016/j.quascirev.2009.11.010, 2010. 5970, 5971, 5972

Leuenberger, M. C.: Modeling the signal transfer of seawater $\delta^{18}\text{O}$ to the $\delta^{18}\text{O}$ of atmospheric oxygen using a diagnostic box model for the terrestrial and marine biosphere, *J. Geophys. Res.*, 102, 26841–26850, doi:10.1029/97JC00160, 1997. 5967

Lipenkov, V. Y., Raynaud, D., Loutre, M. F., and Duval, P.: On the potential of coupling air content and O_2/N_2 from trapped air for establishing an ice core chronology tuned on local insolation, *Quat. Sci. Rev.*, 30, 3280–3289, doi:10.1016/j.quascirev.2011.07.013, 2011. 5968, 5972, 5977, 5978, 6001

Lorius, C., Ritz, C., Jouzel, J., Merlivat, L., and Barkov, N. I.: A 150 000-year climatic record from Antarctic ice, *Nature*, 316, 591–596, doi:10.1038/316591a0, 1985. 5966

CPD

8, 5963–6009, 2012

AICC2012:
120–800 ka

L. Bazin et al.

Title Page

Abstract

Introduction

Conclusions

References

Tables

Figures

◀

▶

◀

▶

Back

Close

Full Screen / Esc

Printer-friendly Version

Interactive Discussion



Loulergue, L.: Contraintes chronologiques et biogeochemiques grace au methane dans la glace naturelle: une application aux forages du projet EPICA, 2007, Ph. D. thesis, UJF, France, 2007. 5972

5 Loulergue, L., Parrenin, F., Blunier, T., Barnola, J.-M., Spahni, R., Schilt, A., Raisbeck, G., and Chappellaz, J.: New constraints on the gas age-ice age difference along the EPICA ice cores, 0–50 kyr, *Clim. Past*, 3, 527–540, doi:10.5194/cp-3-527-2007, 2007. 5972

10 Loulergue, L., Schilt, A., Spahni, R., Masson-Delmotte, V., Blunier, T., Lemieux, B., Barnola, J.-M., Raynaud, D., Stocker, T. F., and Chappellaz, J.: Orbital and millennial-scale features of atmospheric CH₄ over the past 800 000 years, *Nature*, 453, 383–386, doi:10.1038/nature06950, 2008. 5968, 5984, 6007, 6008

Lourantou, A., Chappellaz, J., Barnola, J.-M., Masson-Delmotte, V., and Raynaud, D.: Changes in atmospheric CO₂ and its carbon isotopic ratio during the penultimate deglaciation, *Quat. Sci. Rev.*, 29, 1983–1992, doi:10.1016/j.quascirev.2010.05.002, 2010. 5982

15 Lüthi, D., Le Floch, M., Bereiter, B., Blunier, T., Barnola, J.-M., Siegenthaler, U., Raynaud, D., Jouzel, J., Fischer, H., Kawamura, K., and Stocker, T. F.: High-resolution carbon dioxide concentration record 650 000–800 000 years before present, *Nature*, 453, 379–382, doi:10.1038/nature06949, 2008. 5968

20 Malaizé, B., Paillard, D., Jouzel, J., and Raynaud, D.: The Dole effect over the last two glacial-interglacial cycles, *J. Geophys. Res.*, 104, 14199–14208, doi:10.1029/1999JD900116, 1999. 5966

25 Masson-Delmotte, V., Stenni, B., Blunier, T., Cattani, O., Chappellaz, J., Cheng, H., Dreyfus, G., Edwards, R. L., Falourd, S., Govin, A., Kawamura, K., Johnsen, S. J., Jouzel, J., Landais, A., Lemieux-Dudon, B., Lourantou, A., Marshall, G., Minster, B., Mudelsee, M., Pol, K., Rothlisberger, R., Selmo, E., and Waelbroeck, C.: Abrupt change of Antarctic moisture origin at the end of Termination II, *P. Natl. Acad. Sci. USA*, 107, 12091–12094, doi:10.1073/pnas.0914536107, 2010a. 5982

30 Masson-Delmotte, V., Stenni, B., Pol, K., Braconnot, P., Cattani, O., Falourd, S., Kageyama, M., Jouzel, J., Landais, A., Minster, B., Barnola, J. M., Chappellaz, J., Krinner, G., Johnsen, S., Röthlisberger, R., Hansen, J., Mikolajewicz, U., and Otto-Bliesner, B.: EPICA Dome C record of glacial and interglacial intensities, *Quat. Sci. Rev.*, 29, 113–128, doi:10.1016/j.quascirev.2009.09.030, 2010b. 5984

Masson-Delmotte, V., Buiron, D., Ekaykin, A., Frezzotti, M., Gallée, H., Jouzel, J., Krinner, G., Landais, A., Motoyama, H., Oerter, H., Pol, K., Pollard, D., Ritz, C., Schlosser, E., Sime, L. C.,

CPD

8, 5963–6009, 2012

AICC2012:
120–800 ka

L. Bazin et al.

Title Page

Abstract

Introduction

Conclusions

References

Tables

Figures

◀

▶

◀

▶

Back

Close

Full Screen / Esc

Printer-friendly Version

Interactive Discussion



**AICC2012:
120–800 ka**

L. Bazin et al.

[Title Page](#)

[Abstract](#)

[Introduction](#)

[Conclusions](#)

[References](#)

[Tables](#)

[Figures](#)

◀

▶

◀

▶

[Back](#)

[Close](#)

[Full Screen / Esc](#)

[Printer-friendly Version](#)

[Interactive Discussion](#)



history of the past 420 000 years from the Vostok ice core, Antarctica, *Nature*, 399, 429–436, doi:10.1038/20859, 1999. 5966, 5967, 5968, 6005, 6007

5 Raisbeck, G. M., Yiou, F., Jouzel, J., and Stocker, T. F.: Direct north-south synchronization of abrupt climate change record in ice cores using Beryllium 10, *Clim. Past*, 3, 541–547, doi:10.5194/cp-3-541-2007, 2007. 5966, 5968

10 Rasmussen, S. O., Andersen, K. K., Svensson, A. M., Steffensen, J. P., Vinther, B. M., Clausen, H. B., Siggaard-Andersen, M.-L., Johnsen, S. J., Larsen, L. B., Dahl-Jensen, D., Bigler, M., Röhlisberger, R., Fischer, H., Goto-Azuma, K., Hansson, M. E., and Ruth, U.: A new Greenland ice core chronology for the last glacial termination, *J. Geophys. Res.-Atmos.*, 111, D06102, doi:10.1029/2005JD006079, 2006. 5966

Raynaud, D., Lipenkov, V., Lemieux-Dubon, B., Duval, P., Loutre, M.-F., and Lhomme, N.: The local insolation signature of air content in Antarctic ice. A new step toward an absolute dating of ice records, *Earth Planet. Sci. Lett.*, 261, 337–349, doi:10.1016/j.epsl.2007.06.025, 2007. 5968, 5972, 5977, 6000

15 Ruddiman, W. and Raymo, M.: A methane-based time scale for Vostok ice, *Quat. Sci. Rev.*, 22, 141–155, doi:10.1016/S0277-3791(02)00082-3, 2003. 5966

Ruth, U., Barnola, J.-M., Beer, J., Bigler, M., Blunier, T., Castellano, E., Fischer, H., Fundel, F., Huybrechts, P., Kaufmann, P., Kipfstuhl, S., Lambrecht, A., Morganti, A., Oerter, H., Parrenin, F., Rybak, O., Severi, M., Udisti, R., Wilhelms, F., and Wolff, E.: “EDML1”: a chronology for the EPICA deep ice core from Dronning Maud Land, Antarctica, over the last 150 000 years, *Clim. Past*, 3, 475–484, doi:10.5194/cp-3-475-2007, 2007. 5969, 5972

20 Salamatian, A. N., Tsiganova, E. A., Lipenkov, V. Y., and Petit, J. R.: Vostok (Antarctica) ice-core time-scale from datings of different origins, *Ann. Glaciol.*, 39, 283–292, doi:10.3189/172756404781814023, 2004. 5970

25 Schilt, A., Baumgartner, M., Blunier, T., Schwander, J., Spahni, R., Fischer, H., and Stocker, T. F.: Glacial-interglacial and millennial-scale variations in the atmospheric nitrous oxide concentration during the last 800 000 years, *Quat. Sci. Rev.*, 29, 182–192, doi:10.1016/j.quascirev.2009.03.011, 2010. 5972, 6007

30 Schüpbach, S., Federer, U., Bigler, M., Fischer, H., and Stocker, T. F.: A refined TALDICE-1a age scale from 55 to 112 ka before present for the Talos Dome ice core based on high-resolution methane measurements, *Clim. Past*, 7, 1001–1009, doi:10.5194/cp-7-1001-2011, 2011. 5969, 5972, 5975, 6005, 6007

CPD

8, 5963–6009, 2012

AICC2012:
120–800 ka

L. Bazin et al.

[Title Page](#)

[Abstract](#)

[Introduction](#)

[Conclusions](#)

[References](#)

[Tables](#)

[Figures](#)

◀

▶

◀

▶

[Back](#)

[Close](#)

[Full Screen / Esc](#)

[Printer-friendly Version](#)

[Interactive Discussion](#)



- Schwander, J., Barnola, J.-M., Andrie, C., Leuenberger, M., Ludin, A., Raynaud, D., and Stauffer, B.: The age of the air in the firn and the ice at Summit, Greenland, *J. Geophys. Res.*, 98, 2831–2838, doi:10.1029/92JD02383, 1993. 5970
- Severi, M., Becagli, S., Castellano, E., Morganti, A., Traversi, R., Udisti, R., Ruth, U., Fischer, H.,
5 Huybrechts, P., Wolff, E., Parrenin, F., Kaufmann, P., Lambert, F., and Steffensen, J. P.: Synchronisation of the EDML and EDC ice cores for the last 52 kyr by volcanic signature matching, *Clim. Past*, 3, 367–374, doi:10.5194/cp-3-367-2007, 2007. 5972
- Severi, M., Udisti, R., Becagli, S., Stenni, B., and Traversi, R.: Volcanic synchronisation of
10 the EPICA-DC and TALDICE ice cores for the last 42 kyr BP, *Clim. Past*, 8, 509–517, doi:10.5194/cp-8-509-2012, 2012. 5972
- Severinghaus, J. P. and Battle, M. O.: Fractionation of gases in polar ice during bubble close-off: New constraints from firn air Ne, Kr and Xe observations, *Earth Planet. Sci. Lett.*, 244, 474–500, doi:10.1016/j.epsl.2006.01.032, 2006. 5967
- Severinghaus, J. P., Grachev, A., and Battle, M.: Thermal fractionation of air in polar
15 firn by seasonal temperature gradients, *Geochem. Geophys. Geosyst.*, 2, 1048–1024, doi:10.1029/2000GC000146, 2001. 5973
- Severinghaus, J. P., Beaudette, R., Headly, M. A., Taylor, K., and Brook, E. J.: Oxygen-18 of O₂ records the impact of abrupt climate change on the terrestrial biosphere, *Science*, 324, 1431–1434, doi:10.1126/science.1169473, 2009. 5966
- Severinghaus, J. P., Albert, M. R., Courville, Z. R., Fahnestock, M. A., Kawamura, K.,
20 Montzka, S. A., Mühle, J., Scambos, T. A., Shields, E., Shuman, C. A., Suwa, M., Tans, P., and Weiss, R. F.: Deep air convection in the firn at a zero-accumulation site, central Antarctica, *Earth Planet. Sci. Lett.*, 293, 359–367, doi:10.1016/j.epsl.2010.03.003, 2010. 5973
- Sowers, T., Bender, M., and Raynaud, D.: Elemental and isotopic composition of occluded O₂
25 and N₂ in polar ice, *J. Geophys. Res.*, 94, 5137–5150, doi:10.1029/JD094iD04p05137, 1989. 5973
- Stenni, B., Buiron, D., Frezzotti, M., Albani, S., Barbante, C., Bard, E., Barnola, J. M., Baroni, M., Baumgartner, M., Bonazza, M., Capron, E., Castellano, E., Chappellaz, J., Delmonte, B., Falourd, S., Genoni, L., Iacumin, P., Jouzel, J., Kipfstuhl, S., Landais, A., Lemieux-Dudon, B., Maggi, V., Masson-Delmotte, V., Mazzola, C., Minster, B., Montagnat, M., Mulvaney, R., Narisci, B., Oerter, H., Parrenin, F., Petit, J. R., Ritz, C., Scarchilli, C., Schilt, A., Schüpbach, S., Schwander, J., Selmo, E., Severi, M., Stocker, T. F., and Udisti, R.: Expression of the bipolar
30

[Title Page](#)[Abstract](#)[Introduction](#)[Conclusions](#)[References](#)[Tables](#)[Figures](#)[◀](#)[▶](#)[◀](#)[▶](#)[Back](#)[Close](#)[Full Screen / Esc](#)[Printer-friendly Version](#)[Interactive Discussion](#)

see-saw in Antarctic climate records during the last deglaciation, *Nat. Geosci.*, 4, 46–49, doi:10.1038/ngeo1026, 2011. 6004, 6005, 6007

5 Suwa, M. and Bender, M. L.: Chronology of the Vostok ice core constrained by O₂/N₂ ratios of occluded air, and its implication for the Vostok climate records, *Quat. Sci. Rev.*, 27, 1093–1106, doi:10.1016/j.quascirev.2008.02.017, 2008. 5967, 5968, 5972, 5976, 5978, 6005

10 Svensson, A., Andersen, K. K., Bigler, M., Clausen, H. B., Dahl-Jensen, D., Davies, S. M., Johnsen, S. J., Muscheler, R., Rasmussen, S. O., Röhlisberger, R., Peder Steffensen, J., and Vinther, B. M.: The Greenland ice core chronology 2005, 15 42 kyr, Part 2: comparison to other records, *Quat. Sci. Rev.*, 25, 3258–3267, doi:10.1016/j.quascirev.2006.08.003, 2006. 5966

Svensson, A., Andersen, K. K., Bigler, M., Clausen, H. B., Dahl-Jensen, D., Davies, S. M., Johnsen, S. J., Muscheler, R., Parrenin, F., Rasmussen, S. O., Röhlisberger, R., Seierstad, I., Steffensen, J. P., and Vinther, B. M.: A 60 000 year Greenland stratigraphic ice core chronology, *Clim. Past*, 4, 47–57, doi:10.5194/cp-4-47-2008, 2008. 5966

15 Svensson, A., Bigler, M., Blunier, T., Clausen, H. B., Dahle-Jensen, D., Fischer, H., Fujita, S., Goto-Azuma, K., Johnsen, S. J., Kawamura, K., Kipfstuhl, S., Kohno, M., Parrenin, F., Popp, T., Rasmussen, S. O., Schwander, J., Seierstad, I., Severi, M., Steffensen, J. P., Udisti, R., Uemura, R., Vallelonga, P., Vinther, B. M., Wegner, A., Wilhelms, F., and Winstrup, M.: Direct linking of Greenland and Antarctic ice cores at the Toba eruption (74 kyr BP), *Clim. Past*, this issue, in preparation, 2012. 5972

20 Udisti, R., Becagli, S., Castellano, E., Delmonte, B., Jouzel, J., Petit, J. R., Schwander, J., Stenni, B., and Wolff, E. W.: Stratigraphic correlations between the European Project for Ice Coring in Antarctica (EPICA) Dome C and Vostok ice cores showing the relative variations of snow accumulation over the past 45 kyr, *J. Geophys. Res.-Atmos.*, 109, D08101, doi:10.1029/2003JD004180, 2004. 5972

25 Veres, D., Bazin, L., Landais, A., Lemieux-Dudon, B., Parrenin, F., Martinerie, P., Toyé Mahamadou Kele, H., Capron, E., Chappellaz, J., Rasmussen, S., Severi, M., Svensson, A., Vinther, B., and Wolff, E.: The Antarctic ice core chronology (AICC2012): an optimized multi-parameter and multi-site dating approach for the last 120 thousand years, *Clim. Past*, this issue, 2012. 5970, 5981, 5983

30 Vinther, B., Clausen, H., Kipfstuhl, S., Fischer, H., Bigler, M., Oerter, H., Wegner, A., Wilhelms, F., Sevri, M., Udisti, R., Beer, J., Steinhilber, F., Adolphi, F., Muschler, R., Rasmussen, S., Steffensen, J., and Svensson, A.: A stratigraphic Antarctic chronology covering

CPD

8, 5963–6009, 2012

AICC2012:
120–800 ka

L. Bazin et al.

[Title Page](#)

[Abstract](#)

[Introduction](#)

[Conclusions](#)

[References](#)

[Tables](#)

[Figures](#)

◀

▶

◀

▶

[Back](#)

[Close](#)

[Full Screen / Esc](#)

[Printer-friendly Version](#)

[Interactive Discussion](#)



- the past 16 700 years in the EPICA deep ice core from Dronning Maud Land, in preparation, 2012. 5972
- 5 Wang, Y., Cheng, H., Edwards, R. L., Kong, X., Shao, X., Chen, S., Wu, J., Jiang, X., Wang, X., and An, Z.: Millennial- and orbital-scale changes in the East Asian monsoon over the past 224 000 years, *Nature*, 451, 1090–1093, doi:10.1038/nature06692, 2008. 5966
- Yiou, F., Raisbeck, G. M., Baumgartner, S., Beer, J., Hammer, C., Johnsen, S., Jouzel, J., Kubik, P. W., Lestringuez, J., Stiévenard, M., Suter, M., and Yiou, P.: Beryllium 10 in the Greenland Ice Core Project ice core at Summit, Greenland, *J. Geophys. Res.*, 102, 26783–26794, doi:10.1029/97JC01265, 1997. 5968
- 10 Yuan, D., Cheng, H., Edwards, R. L., Dykoski, C. A., Kelly, M. J., Zhang, M., Qing, J., Lin, Y., Wang, Y., Wu, J., Dorale, J. A., An, Z., and Cai, Y.: Timing, duration, and transitions of the Last Interglacial Asian Monsoon, *Science*, 304, 575–578, doi:10.1126/science.1091220, 2004. 5969

AICC2012:
120–800 ka

L. Bazin et al.

[Title Page](#)

[Abstract](#)

[Introduction](#)

[Conclusions](#)

[References](#)

[Tables](#)

[Figures](#)

◀

▶

◀

▶

[Back](#)

[Close](#)

[Full Screen / Esc](#)

[Printer-friendly Version](#)

[Interactive Discussion](#)



Title Page	
Abstract	Introduction
Conclusions	References
Tables	Figures
◀	▶
◀	▶
Back	Close
Full Screen / Esc	
Printer-friendly Version	
Interactive Discussion	

Table 1. Orbital ages from $\delta^{18}\text{O}_{\text{atm}}$ for EDC.

depth (m)	gas age (ka)	σ (ka)	source
2644.44	363.094	6.0	a
2697.23	389.425	6.0	a
2708.24	398.546	6.0	a
2751.13	408.283	6.0	a
2777.54	427.377	6.0	a
2795.31	435.854	6.0	a *
2812.79	454.779	6.0	a *
2819.2	464.557	6.0	b
2829.36	474.756	6.0	b
2841.75	485.293	6.0	b
2856.27	495.921	6.0	b
2872.56	506.642	6.0	b
2890.33	517.602	6.0	b
2913.3	532.027	6.0	b *
2921.99	545.313	6.0	b
2938.24	556.414	6.0	b
2968.08	567.606	6.0	b
2998.96	578.627	6.0	b
3008.93	589.460	6.0	b
3017.25	600.078	6.0	b
3027.54	610.875	6.0	b
3035.41	622.074	6.0	b
3043.01	634.419	6.0	b
3048.51	649.064	6.0	b
3056.77	660.789	6.0	b
3065.93	671.703	6.0	b
3077.74	682.326	6.0	b
3093.51	693.159	6.0	b
3112.43	703.964	6.0	b
3119.57	714.369	6.0	b
3124.27	724.376	6.0	b
3136.18	733.949	6.0	b
3143.2	741.944	6.0	b
3152.25	749.184	6.0	b
3158.91	758.069	6.0	b
3166.87	767.679	6.0	b
3174.81	777.607	6.0	b
3180.6	787.736	6.0	b
3189.83	797.460	6.0	b

a: this study.

b: Dreyfus et al. (2007). The stars indicate tie-points which have been removed (see Sect. 4.1).



Table 2. Orbital ages from $\delta^{18}\text{O}_{\text{atm}}$ for TALDICE.

depth (m)	gas age (ka)	σ (ka)
668.93	12.060	6.0
1255.55	60.960	6.0
1308.39	72.270	6.0
1333.37	83.870	6.0
1357.95	95.000	6.0
1373.99	105.720	6.0
1390.4	116.500	6.0
1406.27	127.690	6.0

[Title Page](#)[Abstract](#)[Introduction](#)[Conclusions](#)[References](#)[Tables](#)[Figures](#)[|◀](#)[▶|](#)[◀](#)[▶](#)[Back](#)[Close](#)[Full Screen / Esc](#)[Printer-friendly Version](#)[Interactive Discussion](#)

Table 3. Orbital ages from $\delta\text{O}_2/\text{N}_2$ for EDC, deduced from Landais et al. (2012). The stars indicate tie-points which have been removed (see Sect. 4.1).

depth (m)	ice age (ka)	σ (ka)
2795.69	449.000	4.0 *
2808.33	460.000	4.0
2818.15	470.000	4.0
2829.13	480.000	4.0
2841.58	490.000	4.0
2858.78	501.000	4.0
2873.06	512.000	4.0
2888.95	522.000	4.0
2905.88	533.000	4.0
2919.62	551.000	4.0 *
2936.61	562.000	4.0
2975.52	573.000	4.0
2999.23	583.000	4.0
3009.36	594.000	4.0
3017.73	605.000	4.0
3028.6	616.000	4.0
3065.86	677.000	4.0
3078.05	688.000	4.0
3092.52	698.000	4.0
3109.93	710.000	4.0
3169.32	778.000	6.0 *
3179.27	788.000	6.0 *

AICC2012:
120–800 ka

L. Bazin et al.

[Title Page](#)

[Abstract](#)

[Introduction](#)

[Conclusions](#)

[References](#)

[Tables](#)

[Figures](#)

◀

▶

◀

▶

[Back](#)

[Close](#)

[Full Screen / Esc](#)

[Printer-friendly Version](#)

[Interactive Discussion](#)



Table 4. Orbital ages from air content for EDC, deduced from Raynaud et al. (2007).

depth (m)	ice age (ka)	σ (ka)
501.65	21.950	2.879
693.668	38.950	2.211
1255.93	86.950	3.082
1377.67	100.950	4.031
1790.29	142.950	6.468
2086.69	202.950	6.403
2186.29	216.950	6.316
2307.2	245.950	6.316
2350.1	260.950	6.615
2500.25	306.950	6.652
2510.75	318.950	6.242
2610.8	346.950	7.120
2632.25	359.950	6.576
2783.5	424.950	6.782

Table 5. Orbital ages from air content for Vostok, deduced from Lipenkov et al. (2011).

depth (m)	ice age (ka)	σ (ka)
2420.28	191.950	6.663
2488.27	202.950	6.600
2848.45	260.950	7.215
2883.02	275.950	6.343
3011	307.950	6.424
3043.04	318.950	6.308
3145.95	346.950	6.527
3185.46	359.950	6.704

Title Page	Abstract	Introduction
Conclusions	References	
Tables	Figures	
◀	▶	
◀	▶	
Back	Close	
Full Screen / Esc		
Printer-friendly Version		
Interactive Discussion		



Table 6. Comparison of the warm interglacial durations at EDC on the AICC2012 and EDC3 age scales.

Interglacial	EDC EDC3 (ka)	EDC AICC2012 (ka)
MIS 1	0–12.0 (12.0)	0–12.3 (12.3)
MIS 5.5	116.3–132.5 (16.2)	115.5–132.4 (16.9)
MIS 7.5	239.8–244.7 (4.9)	240.8–245.8 (5.0)
MIS 9.3	323.2–336.7 (13.5)	324.6–338.8 (14.2)
MIS 11.3	395.2–426.7 (31.5)	395.5–426.5 (31.0)

[Title Page](#)[Abstract](#)[Introduction](#)[Conclusions](#)[References](#)[Tables](#)[Figures](#)[|◀](#)[▶|](#)[◀](#)[▶](#)[Back](#)[Close](#)[Full Screen / Esc](#)[Printer-friendly Version](#)[Interactive Discussion](#)

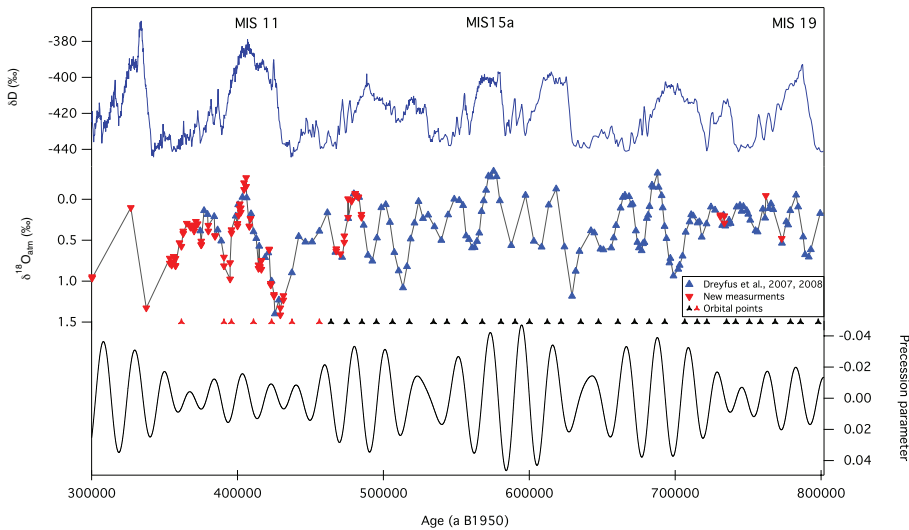


Fig. 1. EDC records between 300 and 800 ka on the EDC3 age scale. Top: water stable isotope (δD) record with labeling of selected interglacial periods (Jouzel et al., 2007). Middle: complete record of $\delta^{18}\text{O}_{\text{atm}}$, blue triangles from Dreyfus et al. (2007, 2008) and red triangles from this study. Bottom: precession parameter (here on a reverse y-axis) obtained with the Analyseries software (Paillard et al., 1996), calculated using the Laskar et al. (2004) solution. Black points indicate the position of tie-points between $\delta^{18}\text{O}_{\text{atm}}$ and precession parameter signals from Dreyfus et al. (2007); the red ones are from this study (Table 1).

[Title Page](#)
[Abstract](#)
[Introduction](#)
[Conclusions](#)
[References](#)
[Tables](#)
[Figures](#)
[|◀](#)
[▶|](#)
[◀](#)
[▶](#)
[Back](#)
[Close](#)
[Full Screen / Esc](#)
[Printer-friendly Version](#)
[Interactive Discussion](#)

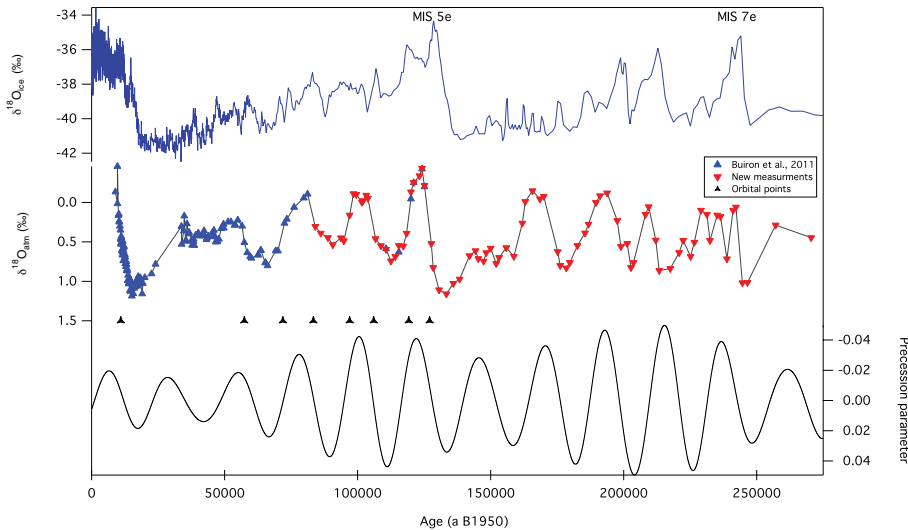



Fig. 2. TALDICE records between 0 and 250 ka on TALDICE 1a age scale. Top: water stable isotope ($\delta^{18}\text{O}_{\text{ice}}$) record with labeling of selected interglacial periods (Stenni et al., 2011). Middle: complete record of $\delta^{18}\text{O}_{\text{atm}}$, blue triangles from Buiron et al. (2011) and red triangles from this study. Bottom: precession parameter (same as in Fig. 1).

- [Title Page](#)
- [Abstract](#) [Introduction](#)
- [Conclusions](#) [References](#)
- [Tables](#) [Figures](#)
- [◀](#) [▶](#)
- [◀](#) [▶](#)
- [Back](#) [Close](#)
- [Full Screen / Esc](#)
- [Printer-friendly Version](#)
- [Interactive Discussion](#)



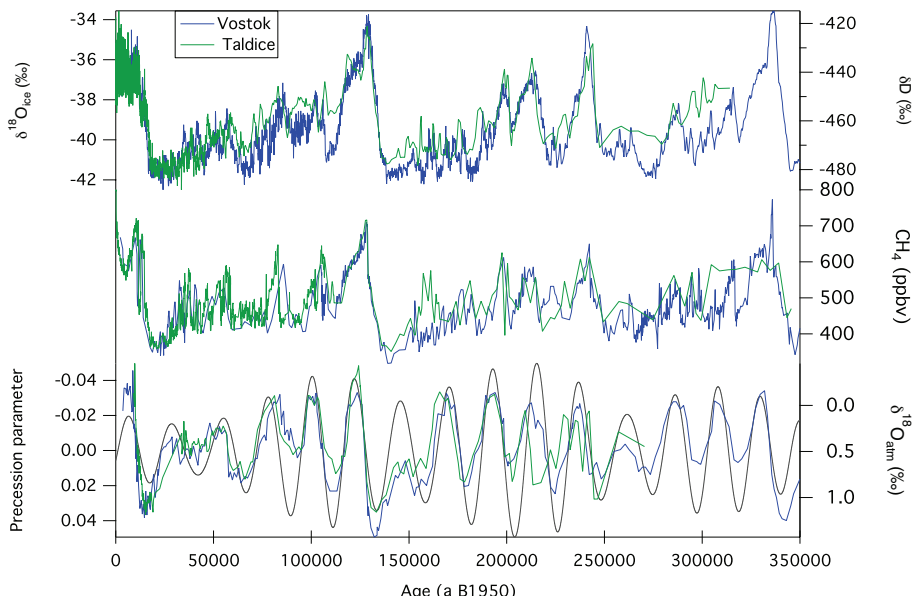


Fig. 3. Comparison between Vostok (blue) and TALDICE (green) ice cores on the $\delta^{18}\text{O}_{\text{atm}}$ chronology (Bender, 2002) and TALDICE 1a age scale (Buiron et al., 2011; Schüpbach et al., 2011) respectively. Top: water stable isotope records (δD and $\delta^{18}\text{O}_{\text{ice}}$ respectively) (Petit et al., 1999; Stenni et al., 2011). Middle: methane records, Vostok: Petit et al. (1999); Caillon et al. (2003); Delmotte et al. (2004), TALDICE: Buiron et al. (2011); Schüpbach et al. (2011). Bottom: $\delta^{18}\text{O}_{\text{atm}}$ records: Vostok: Bender (2002); Suwa and Bender (2008), TALDICE: Buiron et al. (2011) and this study. The grey curve corresponds to the precession parameter.

Title Page	Abstract	Introduction
Conclusions	References	
Tables	Figures	
◀	▶	
◀	▶	
Back	Close	
Full Screen / Esc		
Printer-friendly Version		
Interactive Discussion		

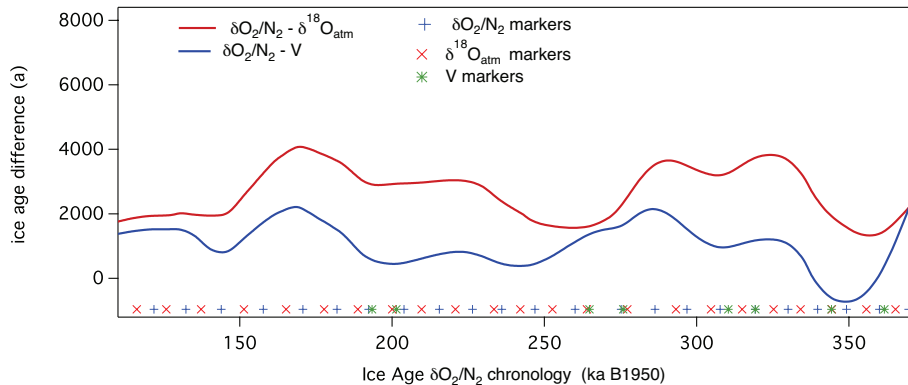


Fig. 4. Ice age difference between the $\delta\text{O}_2/\text{N}_2$ and air content (V) chronologies (blue) and $\delta\text{O}_2/\text{N}_2$ and $\delta^{18}\text{O}_{\text{atm}}$ chronologies (red) on the Vostok ice core. The different markers show the position of the orbital age constraints for each chronology.

Title Page	Abstract	Introduction
Conclusions	References	
Tables	Figures	
◀	▶	
◀	▶	
Back	Close	
Full Screen / Esc		
Printer-friendly Version		
Interactive Discussion		



AICC2012:
120–800 ka

L. Bazin et al.

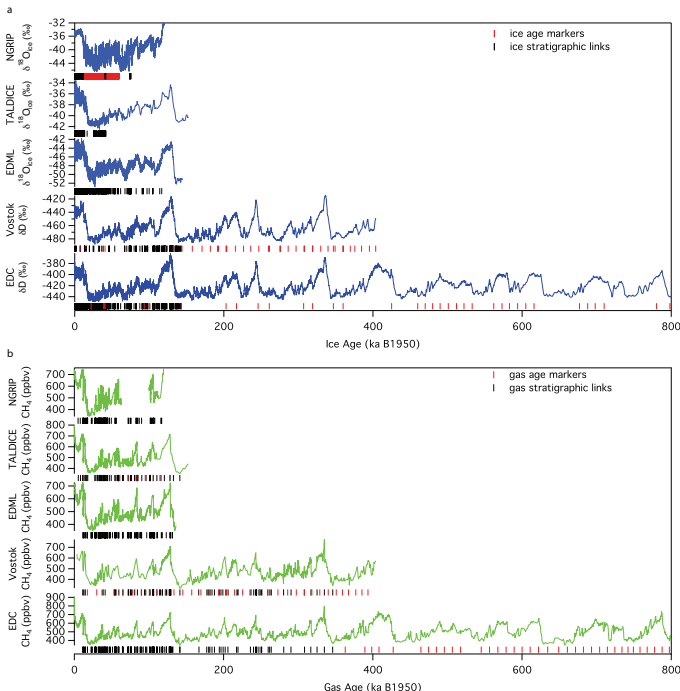


Fig. 5. (a) Water stable isotope records of NGRIP (NorthGRIP Community Members, 2004), TALDICE (Stenni et al., 2011), EDML (EPICA Community Members, 2006, 2010), Vostok (Petit et al., 1999) and EDC (Jouzel et al., 2007) on the AICC2012 age scale. **(b)** Methane records of NGRIP (Greenland composite: Capron et al. (2010); EPICA Community Members (2006); Flückiger et al. (2004); Huber et al. (2006); Schilt et al. (2010)), TALDICE (Buiron et al., 2011; Schüpbach et al., 2011), EDML (EPICA Community Members, 2006), Vostok (Caillon et al., 2003; Delmotte et al., 2004; Petit et al., 1999) and EDC (Loulergue et al., 2008) on the AICC2012 age scale. Stratigraphic links and age markers positions are displayed under each core.

Title Page	Abstract	Introduction
Conclusions	References	
Tables	Figures	
◀	▶	
◀	▶	
Back	Close	
Full Screen / Esc		
	Printer-friendly Version	
	Interactive Discussion	



AICC2012:
120–800 ka

L. Bazin et al.

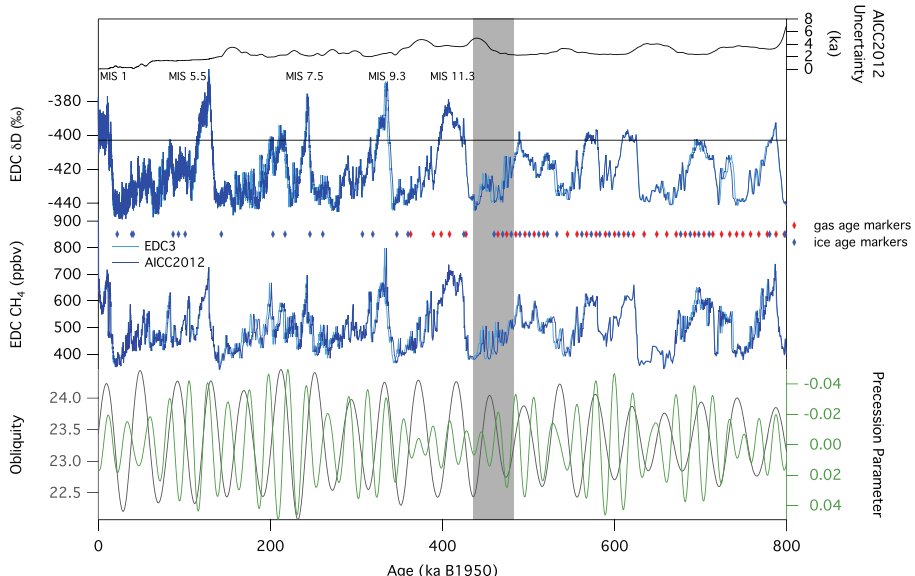


Fig. 6. Top: EDC AIICC2012 chronology uncertainty. EDC deuterium records (EPICA Community Members, 2004) over the last 800 ka on the EDC3 (light blue) and AIICC2012 (dark blue) age scales. The horizontal line corresponds to -403\% and limits the interglacial periods (EPICA Community Members, 2004). The position of the orbital markers is shown in the gas (red markers) and ice (blue markers). Middle: CH_4 records of EDC (Loulergue et al., 2008) on EDC3 (light blue) and AIICC2012 (dark blue). Bottom: obliquity (grey) and precession parameter (green) over the last 800 ka, obtained with Analyseries software (Paillard et al., 1996). The shaded zone highlights the period of significant differences between the two chronologies.

Title Page

Abstract

Introduction

Conclusion

References

Tables

Figures

◀

▶ |

Back

Close

Full Screen / Esc

[Printer-friendly Version](#)

Interactive Discussion



AICC2012:
120–800 ka

L. Bazin et al.

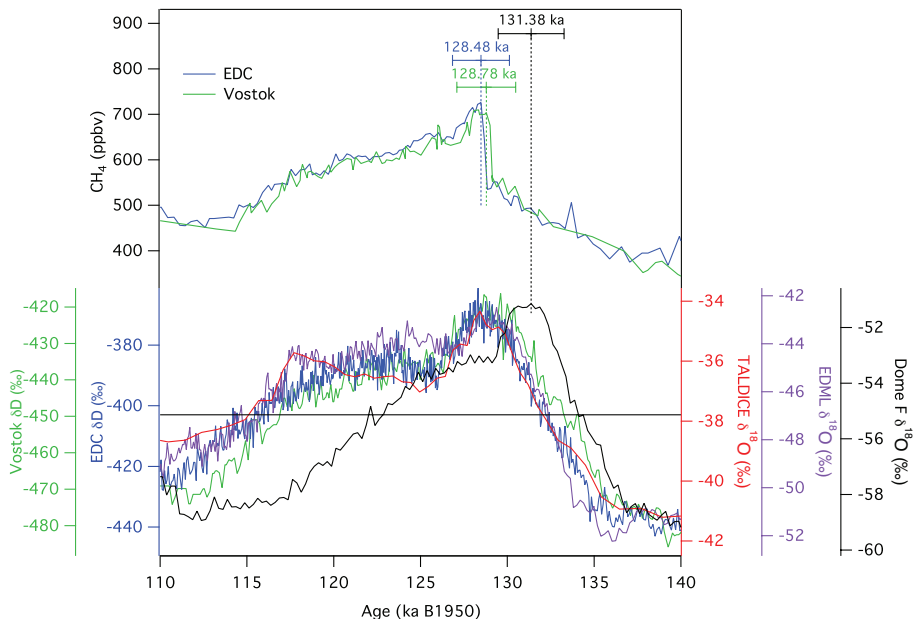


Fig. 7. Bottom: comparison of MIS 5.5 duration in several ice cores. The EDC, Vostok, EDML and TALDICE isotopic records are on AICC2012 age scales. The Dome F $\delta^{18}\text{O}$ is on the DFO-2006 chronology (Kawamura et al., 2007). The black horizontal line corresponds to the -403 ‰ interglacial threshold on EDC. Top: methane records of Vostok and EDC. Termination II ages are defined from the timing of the sharp methane rise for EDC (blue) and Vostok (green), and the water stable isotope optima for Dome F (black).

- [Title Page](#)
- [Abstract](#) [Introduction](#)
- [Conclusions](#) [References](#)
- [Tables](#) [Figures](#)
- [◀](#) [▶](#)
- [◀](#) [▶](#)
- [Back](#) [Close](#)
- [Full Screen / Esc](#)
- [Printer-friendly Version](#)
- [Interactive Discussion](#)

